JOURNAL OF BACTERIOLOGY, Feb. 1992, p. 832–840
0021-9193/92/030832-09$02.00/0

Vol. 174, No. 3

Morphology and Dynamics of Protruding Spirochete Periplasmic Flagella

NYLES W. CHARON,[1]* STUART F. GOLDSTEIN,[2] STEVEN M. BLOCK,[3] KRISTINA CURCI,[1] JOHN D. RUBY,[1] JILL A. KREILING,[1] AND RONALD J. LIMBERGER[1,4]

Department of Microbiology and Immunology, West Virginia University, Health Sciences Center North, Morgantown, West Virginia 26506[1]; Department of Genetics and Cell Biology, University of Minnesota, St. Paul, Minnesota 55108[2]; Rowland Institute for Science, Cambridge, Massachusetts 02142[3]; and Wadsworth Center for Laboratories and Research, New York State Department of Health, Albany, New York 12201-0509[4]

Received 11 October 1991/Accepted 22 November 1991

We recently characterized the three-dimensional shape of *Treponema phagedenis* periplasmic flagella (PFs). In the course of these studies, we observed protrusions on swimming cells that resembled PFs. Here we present a detailed characterization of the shape, structure, and motion of these protrusions. Although protrusion formation occurred primarily in wild-type cells during the stationary phase, a large fraction of exponential-phase cells of cell cylinder helicity mutants (>90% of mutant T-52) had protrusions. These results suggest that cells bearing protrusions can still participate in cell division. *T. phagedenis* protrusions had the identical helix handedness, pitch, and diameter to those of purified PFs. Protrusions were not present on mutants unable to synthesize PFs, but were present in all motile revertants which regained PFs. These results, taken together with electron microscope observations, suggest that protrusions consist of PFs surrounded by an outer membrane sheath. To analyze protrusion movements, we held cells against a coverglass surface with optical tweezers and observed the motion of protrusions by video-enhanced differential interference contrast light microscopy. Protrusions were found to gyrate in both clockwise and counterclockwise directions, and direct evidence was obtained that protrusions rotate. Protrusions were also observed on *Treponema denticola* and *Borrelia burgdorferi*. These were also left-handed and had the same helix handedness, pitch, and diameter as purified PFs from their respective species. The PFs from *T. denticola* had a helix diameter of 0.26 μm and a helix pitch of 0.78 μm; PFs from *B. burgdorferi* had a helix diameter of 0.28 μm and a helix pitch of 1.48 μm. Protrusions from these spirochete species had similar structures and motion to those of *T. phagedenis*. Our results present direct evidence that PFs rotate and support previously proposed models of spirochete motility.

Spirochetes are a morphologically distinct group of bacteria (12, 27, 40, 49). Outermost is a membrane sheath, and within this sheath is a helical cell cylinder (12, 27). Attached subterminally at each end of the cell cylinder are the periplasmic flagella (PFs) (also referred to as axial filaments, axial fibrils, or endoflagella [11, 27, 31]), which are located between the membrane sheath and cell cylinder. Each PF is attached to only one end of the cell. The PFs extend backward toward the middle of the cell and may overlap in the center. The size of the spirochetes, the number of PFs attached at each end, and whether the PFs overlap in the center of the cell are characteristics that vary from species to species (12, 27).

There are two current models of spirochete motility (3, 4, 23). A key element to both models, which has not been directly tested, is the assumption that PFs rotate in a manner similar to flagella of rod-shaped bacteria (6, 32–34, 43) but in the periplasmic region between the cell cylinder and outer membrane sheath. According to one model, as described for *Spirochaeta aurantia*, rotation of the PFs causes the cell cylinder to roll in one direction and the outer membrane sheath to rotate in the opposite direction (3). Both translating and nontranslating cells are observed: the PFs of translating cells are believed to rotate in the same direction, whereas those of nontranslating cells are believed to rotate in opposite directions (20, 21). (We adopt a frame of reference in which a swimming cell is viewed from the outside, looking from the posterior toward the anterior end.)

The members of the family *Leptospiraceae* are believed to swim by a mechanism somewhat different from that proposed for *S. aurantia* (4, 23). These spirochetes contain one short PF at each end of a right-handed cell cylinder (a right-handed helix spirals clockwise [CW]), and a left-handed helix spirals counterclockwise [CCW], moving away from an observer). The shape of the cell end is determined by the shape and direction of rotation of the PFs; the PFs are assumed to be more rigid than the right-handed (13) cell cylinder. CCW rotation of a PF causes the anterior end to be spiral shaped and the posterior end to be hook shaped. In translating cells, the PFs at both ends are believed to rotate in the same direction. CCW rotation of the anterior PF causes the generation of a gyrating, spiral-shaped wave (i.e., propagating a helical wave motion without necessarily rotating, as a bent wire rotating in a rubber tube is described by Taylor [47]). This wave is sufficient to propel the cells forward in a pure liquid medium. The right-handed cell cylinder concomitantly rolls around the PFs in the opposite direction (CW), which allows the cell to literally screw through a gellike medium with little slippage. Nontranslating cells are believed to have the PFs rotating in opposite directions. Recent evidence supports this model for the family *Leptospiraceae* (10, 14, 24) and *Treponema phagedenis* (15). However, *T. phagedenis* differs from the family *Leptospiraceae* in that *T. phagedenis* translates very poorly

* Corresponding author.

in a pure liquid medium and thus requires a gellike medium for directed movement (48).

We recently determined the three-dimensional shapes of *T. phagedenis* cells and purified PFs (15). Whereas cells were right-handed with bent ends, PFs were left-handed, relatively short, and with a smaller helix diameter and pitch (15). In the process of characterizing *T. phagedenis* cells and PFs, we observed helical protrusions gyrating on a small fraction of motile *T. phagedenis* cells. Sporadic reports of protrusions have appeared in the literature, going back several decades (19, 25, 26, 31, 35, 37–39, 44), but their morphology and dynamics have not been analyzed in detail.

In the present study, we characterize protrusions from *T. phagedenis* by using dark-field and video-enhanced differential interference contrast (DIC) light microscopy (9), optical tweezers (8), and electron microscopy and compare these structures with purified PFs. Video-enhanced DIC light microscopy facilitates maximal resolution of viable cells (9); the optical tweezers enabled us to hold individual cells against a coverglass surface and video-record cell movements for a prolonged interval. We also determined the helical structure of the PFs of *Treponema denticola* and *Borrelia burgdorferi* and analyzed the protrusions from these spirochetes in a similar manner. We present evidence that protrusions have the same helix handedness, pitch, and diameter as purified PFs from a given species and are surrounded by a membrane sheath. We also present direct evidence that PFs rotate.

MATERIALS AND METHODS

Organisms and culture conditions. The origin and description of wild-type *T. phagedenis* Kazan 5; *T. phagedenis* Reiter; PF-deficient motility mutants derived from *T. phagedenis* Kazan 5, T-40 and T-55; and six motility revertants have been previously reported (15, 30). Cell cylinder helicity mutants of *T. phagedenis* Kazan 5, T-52 and T-59, were isolated after nitrosoguanidine mutagenesis as small colony formers by using the same procedure as described for T-40 and T-55 (30). *T. phagedenis* cells were propagated in peptone-yeast extract glucose medium supplemented with 10% rabbit serum (30). *T. denticola* ATCC 33520 was obtained from the American Type Culture Collection and was grown in NOS medium, as described by Leschine and Canale-Parola (29). Growth was monitored by using a model 7 photonephelometer (Coleman Instruments Inc., Oak Brook, Ill.) with readings correlated to cell counts. *B. burgdorferi* 297 was obtained from R. C. Johnson, University of Minnesota, Minneapolis, and grown in BSKY II medium (1). Growth was monitored by direct counts with a Petroff-Hausser counting chamber. Because spirochete media contain rabbit serum, particulate matter in the media was evident in microscopic studies.

PF isolation. The method of isolating *T. phagedenis* PFs has been described previously (30). *T. denticola* and *B. burgdorferi* PFs were isolated by the same method or that of Cockayne et al. (17). The purity of the PF preparations was confirmed by sodium dodecyl sulfate-polyacrylamide gel electrophoresis (30) and dark-field and electron microscopy (15, 30). PFs from *T. phagedenis* wild-type and T-52 and T-59 mutant cells appeared identical with respect to protein composition as revealed by gel electrophoresis and by shape as determined by measurements of helix handedness, pitch, and diameter.

Light microscopy. Cells and purified PFs were examined by high-magnification dark-field microscopy (15, 24). For dark-field microscopy, protrusions and PFs were best visualized with a minimum of fluid. Approximately 5 μl of unwashed cells in growth medium, or PFs in methylcellulose (15), were deposited on the middle of a slide and covered with a 22-mm square coverglass supported with silicone grease on two of the edges. Dark-field video microscopy was carried out as previously described by using either a Sony Model XC-77 or DAGE-MTI model 72 CCD camera (15). Protrusion and PF measurements (helix pitch and diameter) were carried out as previously reported (15). The methods for video-enhanced DIC light microscopy and optical tweezers have been described elsewhere (8, 9). Hard-copy images were prepared by using a Sony UP-850 video graphic printer (9). To estimate the frequency of cell protrusions, we examined 30 cells by dark-field microscopy at several time points during a growth curve and determined the fraction of cells with protrusions at one or both ends. In certain instances, methylcellulose was added to the medium (4, 16, 24).

Electron microscopy. Observations were made with a JEOL 100CX or a Philips 300 microscope, and PF length was determined as previously described (15). To view cells with protrusions, we centrifuged cells, resuspended them in water (or balanced salt solution for *B. burgdorferi*), and stained them with 2% uranyl acetate.

RESULTS

Light and electron microscope analysis of protrusions of *T. phagedenis*. *T. phagedenis* cells were examined by light microscopy during all phases of growth. The bent ends typical of the wild type were clearly evident by video-enhanced DIC light microscopy (Fig. 1a). Approximately 3 to 6% of exponential-phase cells showed protrusions (Fig. 1b), and in stationary-phase cells (5-day-old cultures) this frequency increased to 25%. Exponential-phase cells of helicity mutants had a higher frequency of protrusions than did the wild type. For example, more than 90% of cells of mutant T-52 displayed one or more protrusions during the exponential phase; this mutant has a relatively straight cell body (Fig. 1c). Mutant T-59, which has a greater helix diameter than the wild type (Fig. 1d), had protrusions in 30 to 50% of the cells. Both mutants had generation times approximately the same as the wild type (ca. 11 h).

The position of the protrusions relative to the cell body was characterized in detail. Cell protrusions extended out from the ends of the cells (Fig. 1b and c), outward between dividing cells at the point of division (Fig. 1d), and as a helical thread between dividing cells (Fig. 1e). Protrusions on single cells were at one (Fig. 1b and c) or both ends. On some cells, more than one protrusion was evident on a cell end, and occasionally the protrusions had balloonlike bulges at their tips (Fig. 1f and g; see also Fig. 5). The balloonlike characteristic occurred more frequently in the mutant cells than in the wild type.

Microscopic and genetic analysis indicated that *T. phagedenis* PFs are involved in protrusion structure. Protrusions of the wild type and cell cylinder mutants were helical and left-handed. Protrusions had an identical helix pitch and diameter, and similar length, as purified PFs (Table 1). Genetic evidence that protrusions are associated with PFs was obtained by examination of the PF-deficient mutants T-40 and T-55 (15, 30). No protrusions were detected in either mutant (more than 100 cells were examined for each mutant), whereas all six spontaneously occurring motility revertants regained both PFs and protrusions. Electron

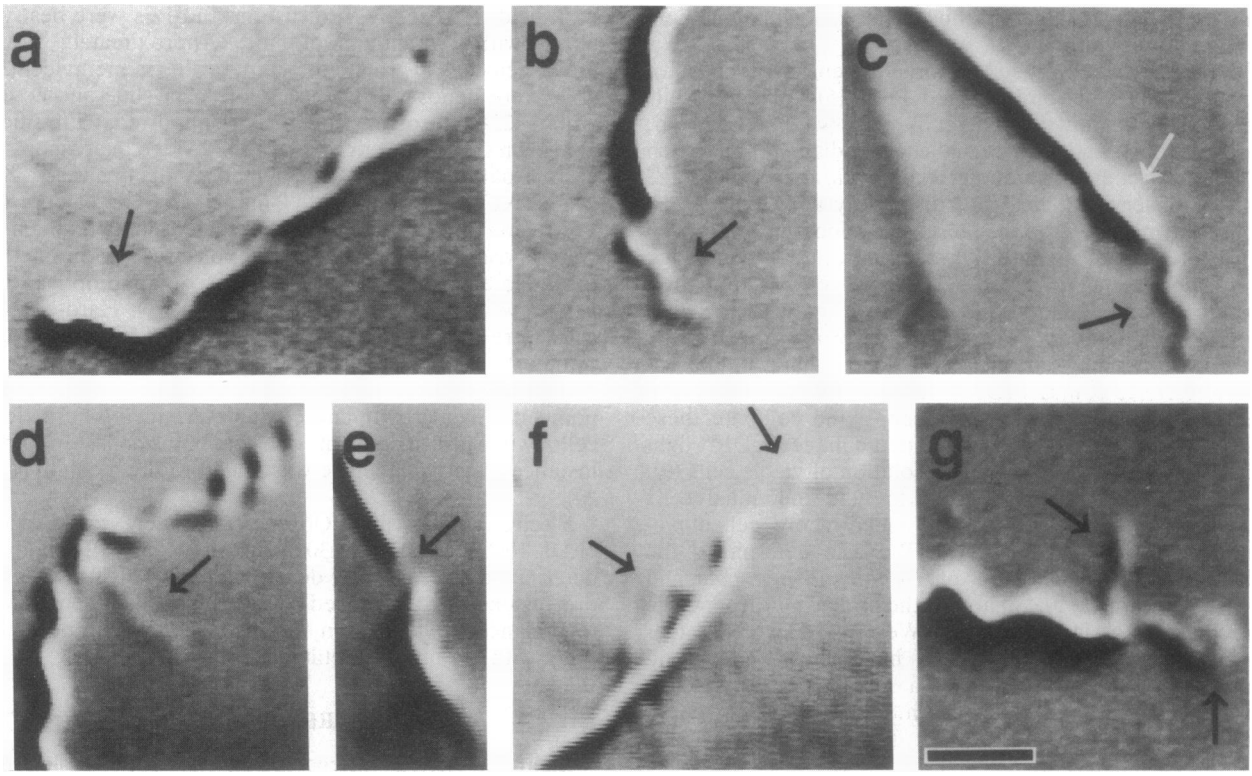

FIG. 1. Video-enhanced DIC images of *T. phagedenis* illustrating (a) a wild-type cell with a bent end (arrow), (b) a wild-type cell with a helical protrusion at one end (arrow), (c) mutant T-52 with a terminal protrusion (dark arrow) (the cell was pinned to the coverglass with optical tweezers [light arrow]), (d) mutant T-59 with the protrusion extending outward between daughter cells (arrow), (e) a wild-type cell with a protrusion between daughter cells (arrow), and (f) wild-type and (g) mutant T-59 with two protrusions at each end, with one protrusion on each cell carrying a balloonlike bulge. Bar, 2 μm.

microscopy revealed that the protrusions consisted of bundles of PFs surrounded by a membrane sheath (Fig. 2a). Not all the PFs protruded at some cell ends; PFs were often also observed to extend backward along the cell body. Taken together, these results indicate that PFs are a component of and contribute significantly to the ultrastructure and shape of spirochete protrusions.

Motion of *T. phagedenis* protrusions. The motion of the protrusions was analyzed in detail. When the cells adhered spontaneously to a glass surface or were held against a glass surface by optical tweezers, the protrusions displayed motion while the cell body remained stationary. Protrusions could gyrate, propagating CW or CCW helical waves (Fig. 3), stop, and reverse direction. The axis of wave propagation was generally not parallel to the helix axis of the protrusion; rather, gyrating protrusions traced out a conical sweep. Some protrusions were seen to trace a wide circular path, as viewed from above, similar to an arm on a clock (not shown). However, the direction of wave propagation was parallel to the helix axis of the protrusion when it was stuck to a glass surface at its tip or when cells were suspended in medium containing in 0.5% methylcellulose. Methylcellulose affects macroscopic viscosity and apparently increases the resistance to lateral slippage of the protrusions, consistent with the observations of Berg and Turner (5). Tiny particles present in the medium occasionally adhered to the protrusions. These particles sometimes moved up or down the protrusion (Fig. 4) and even into the cell body. The movement of these particles suggests that the surface of the protrusions is fluid. These results are consistent with the electron-microscopic observation that the protrusions are PFs surrounded by a membrane sheath.

Protrusions could generate rotational motion. Balloonlike bulges were observed at the tip of some protrusions. In some cases, asymmetric knobs appeared on the bulges, allowing angular orientation to be monitored. Such knobs were clearly observed rotating around the protrusion, passing above and below the focal plane (Fig. 5). Concomitant with this rotation, helical wave propagation occurred along the length of the protrusion. As can be seen from Fig. 5, the

TABLE 1. Comparison of PFs and cell protrusions[a]

Bacterium and structure	Helix diam (μm)	Helix pitch (μm)	Length (μm)
T. phagedenis			
PFs[b]	0.36 ± 0.05	1.26 ± 0.08	2.40 ± 0.66
Protrusions	0.36 ± 0.12	1.27 ± 0.21	2.90 ± 0.58
T. denticola			
PFs	0.26 ± 0.04	0.78 ± 0.09	5.66 ± 1.61
Protrusions	0.21 ± 0.01	0.75 ± 0.06	6.43 ± 1.40
B. burgdorferi			
PFs	0.28 ± 0.03	1.48 ± 0.03	>5
Protrusions	0.30 ± 0.02	1.56 ± 0.07	ND[c]

[a] $n > 20$ for each measurement. Results are expressed as mean ± standard deviation. PFs and protrusions from each species were left-handed.
[b] Measurements of *T. phagedenis* PFs were taken from reference 15.
[c] ND, not determined.

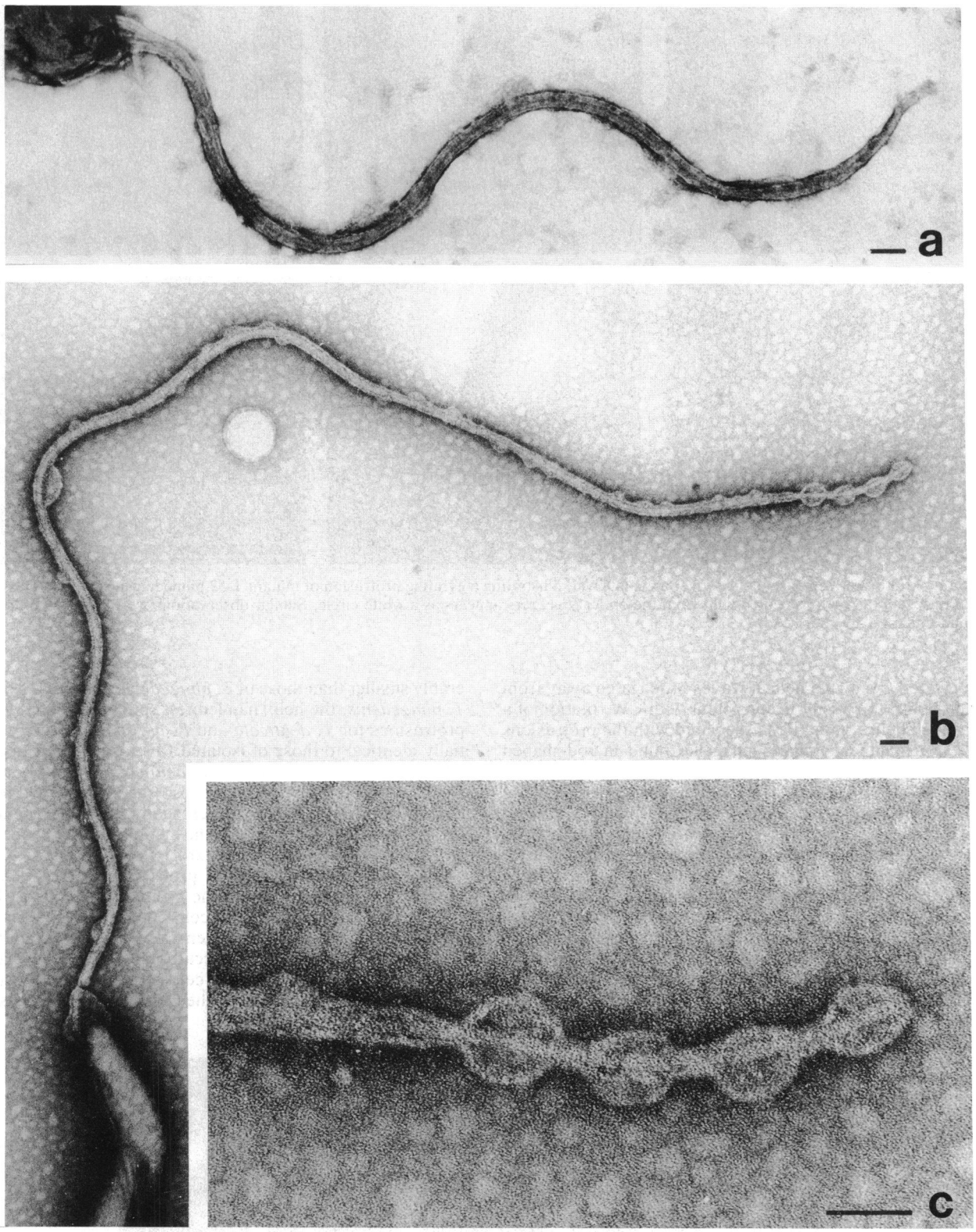

FIG. 2. (a) Electron micrograph of a *T. phagedenis* wild-type cell with a protrusion. Note the membrane around two protruding PFs. (b) Electron micrograph of a *T. denticola* cell with a protrusion. Note that the protrusion has one PF and that two PFs extend backward along cell body. (c) Enlargement of the tip of the protrusion illustrating dissociation of the membrane sheath from the PF. Bar, 0.1 μm.

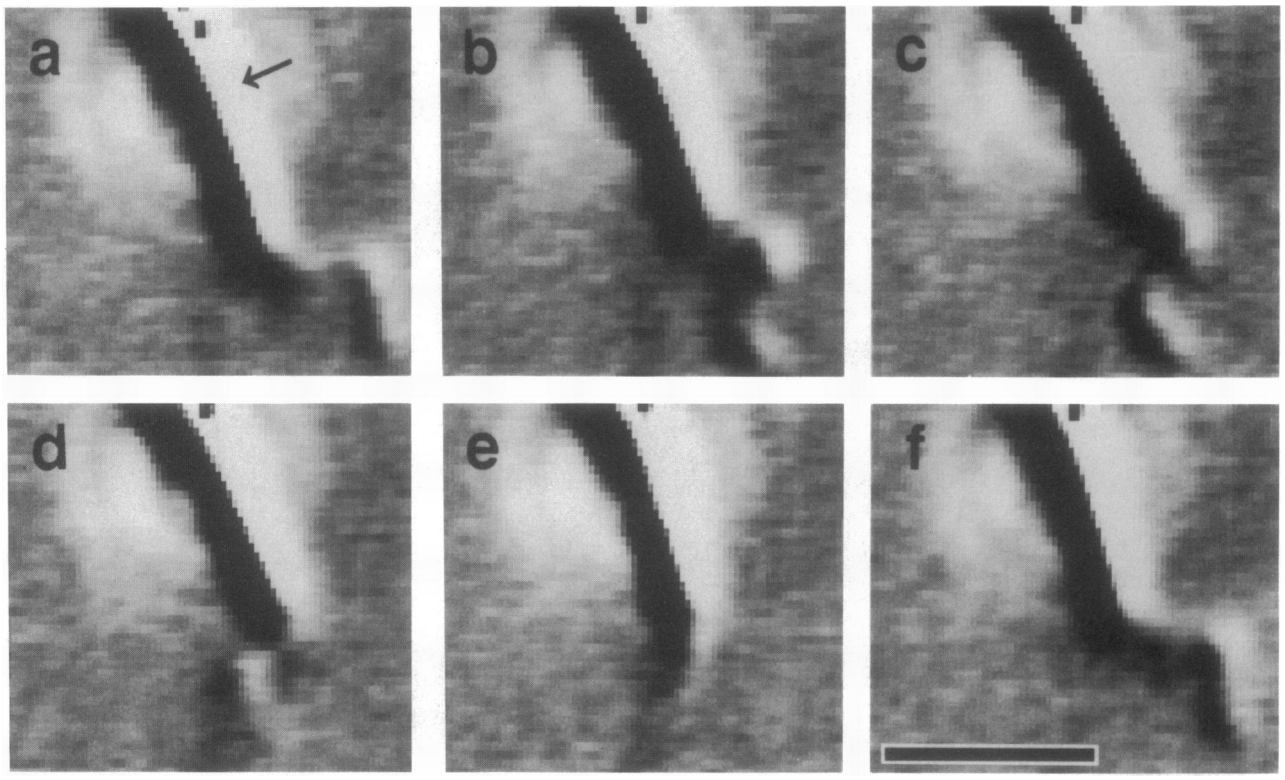

FIG. 3. Multiframe video sequence, over a 2-s interval, illustrating a gyrating protrusion of mutant T-52 pinned against a coverglass with optical tweezers (arrow). Reflected light from the optical tweezers appears as a white circle. Similar observations were made with the wild type and mutant T-59. Bar, 2 μm.

knob rotated CW while helical waves propagated away from the cell body; this result is consistent with CW rotation of a left-handed helix. Thus, PFs associated with the protrusions rotate in a manner similar to flagella found in rod-shaped bacteria.

Analysis of protrusions from other spirochetes. Several other spirochetes were examined for protrusions. *T. phagedenis* Reiter, *T. denticola* (Fig. 6a), and *B. burgdorferi* (Fig. 6b) all had helical protrusions. Protrusions occurred most frequently during the stationary phase of growth and were positioned on the cell body analogously to those of *T. phagedenis*. To compare protrusions with PFs, we characterized the PFs of *T. denticola* and *B. burgdorferi* (28, 42). Purified PFs from both species were left-handed and had a characteristic helix pitch and diameter (Table 1). The helix pitch and diameter of the PFs for *T. denticola* were considerably smaller than those of *T. phagedenis* (Table 1). As with *T. phagedenis*, the helix handedness, pitch, and diameter of protrusions for *T. denticola* and *B. burgdorferi* were essentially identical to those of isolated PFs for the same species (Table 1). The protrusions of *T. denticola* (Fig. 2b) and *B. burgdorferi* were PFs that were also surrounded by a membrane, as shown by electron microscopy. However, near the tip of *T. denticola* protrusions, the membrane often appeared dissociated from the PFs (Fig. 2b).

We analyzed the motion of protrusions of these spirochetes. Wave propagation of the protrusions occurred both toward and away from the cell body for *T. denticola*. Protrusions in *B. burgdorferi* generally appeared stationary relative to the cell body, but occasionally wave propagation was observed independently of cell motion. In contrast to *T. phagedenis*, gyration around the protrusion helix axis, as

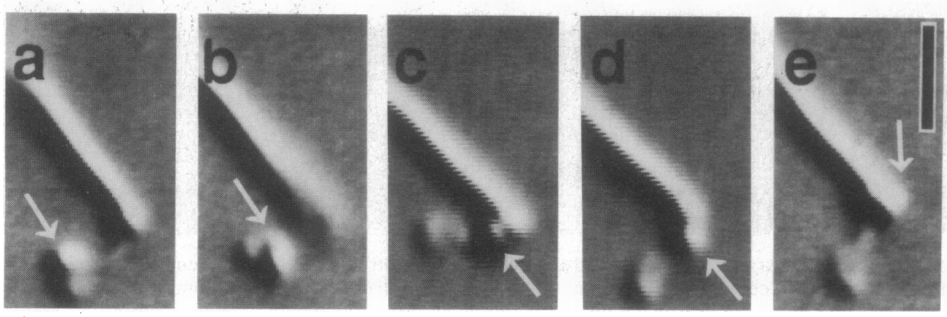

FIG. 4. Multiframe sequence of a 5-s interval illustrating a small particle (white arrow) moving up a protrusion of mutant T-52 from the balloonlike bulge at the distal end toward the cell body. The particle remained attached to the distal end of the cell cylinder. Bar, 2 μm.

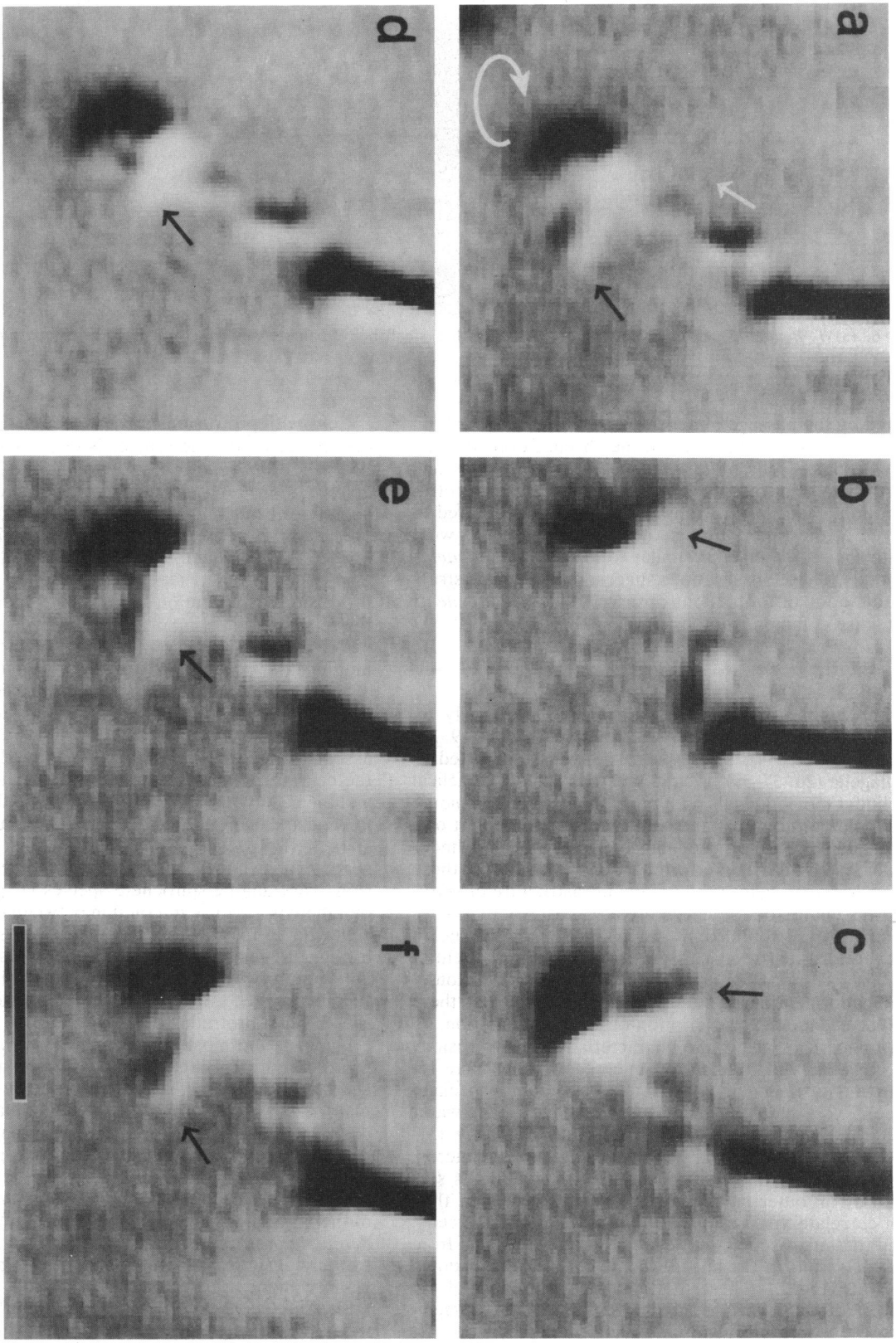

FIG. 5. A multiframe video sequence over a 2-s interval illustrating the rotation of the knob on the balloonlike bulge at the tip of a protrusion of mutant T-52. Note that the knob (dark arrow) rotates clockwise as seen from the top of the figure (white circular arrow), concomitant with helical wave propagation away from the cell body (direction shown by light arrow). The plane of focus is slightly above the protrusion, and the left-handed nature of the helix is clearly discernible in frames a, d, and e. Bar, 2 μm.

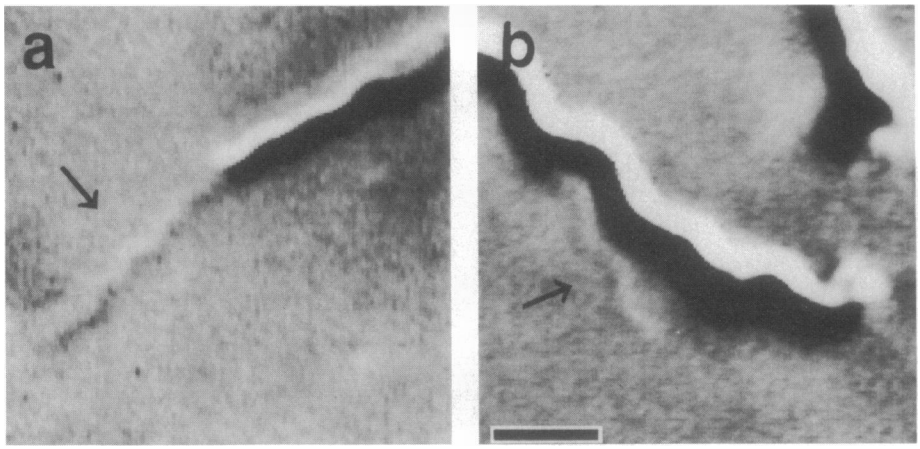

FIG. 6. (a) *T. denticola* cell end showing protrusion with a small helix diameter and pitch (arrow); (b) *B. burgdorferi* cell end with protrusion (arrow). Bar, 2 μm.

indicated by the passage of helical waves, was seen for both *T. denticola* and *B. burgdorferi* in the absence of methylcellulose. On some cells of *T. denticola*, the protrusions had kinks in their helix, and these kinks gyrated during protrusion motion. Many protrusions of *T. denticola* appeared to be frayed at the tips. Particles attached at these tips were found to rotate in a manner similar to that of *T. phagedenis* protrusions. These observations suggest that the basic structure and motion of protrusions observed with *T. phagedenis* Kazan 5 are common to other spirochetal species.

DISCUSSION

Spirochetal protrusions have been noted previously by dark-field, phase-contrast, and electron microscopy (19, 25, 26, 31, 35, 37–39, 44). These protrusions were reported as being flagella (26, 37–39) or simply extensions of the helical cell cylinder (36, 45). Cells with protrusions were commonly noted in old cultures (25) and were believed to be part of a spirochetal life cycle, proceeding from a helical cell cylinder to a final spherical cystlike form (19, 25, 26). Most of these studies were done before the unique ultrastructure of spirochetes was understood, e.g., before it was known that these organisms are surrounded by an outer membrane sheath (27). Therefore, early investigators were unable to identify clearly the nature of the protrusions. Except for Morton et al. (35), who mention that these structures undulate, there has never been a clear description of protrusion motion.

One concern is that some characteristics of protrusions that were observed by electron microscopy may have resulted from artifacts in specimen preparation, especially since cells were centrifuged and suspended in distilled water or buffer before staining. Listgarten and Socransky (31) observed protrusions in oral treponemes by electron microscopy. They also found that the protrusions were PFs surrounded by an outer membrane sheath (31); however, they did not correlate their results with observations of live cells. We find that microscopic particles, probably picked up from the rabbit serum in the medium, can move up and down protrusions (Fig. 4). These motions are reminiscent of the movement of antibody-coated latex beads attached to members of the *Leptospiraceae* (14, 16, 22) and indicate that protrusions have a fluid surface. They are also consistent with the notion that PFs are surrounded by an outer membrane sheath.

Cells with protrusions are not necessarily end-stage, nondividing cells. In wild-type cells of *T. phagedenis*, *T. denticola*, and *B. burgdorferi*, protrusions can generate considerable motion, suggesting that these cells are at least energetically intact. Protrusions occurred with a high frequency during the exponential growth phase of *T. phagedenis* cell helicity mutants T-52 and T-59. Such high frequencies of occurrence (>90% for mutant T-52) imply that protrusions can occur on cells capable of division and are not the result of cell aging or death.

Cell cylinder shape is an important factor for translational motility and protrusion formation. *T. phagedenis* mutants T-52 and T-59 were isolated on the basis of small colony formation on swarm agar plates and are deficient in translational motility. The bent ends of wild-type *T. phagedenis* are associated with short PFs that do not overlap in the center of the cell (15). A close interaction between the rotating PFs and the cell cylinder is believed to cause the ends of the cell to bend and be motile (15). We find that the PFs from a given spirochete species have a well-defined handedness and shape (Table 1). Because both PF and cell cylinder dimensions vary among spirochete species (12, 27), we conclude that there is a critical interaction between the helical PFs and cell cylinder for good motility. The results with *T. phagedenis* suggest that the cell cylinder requires a specific helical configuration to interact properly with the rotating helical PFs; otherwise, the PFs surrounded by the outer membrane sheath often protrude.

Our data are most consistent with a model in which the protruding PFs rotate. Not only do protrusions gyrate, but also asymmetric bulges present on some protrusions of *T. phagedenis* rotate around the longitudinal axis, with concomitant wave propagation down the length of the protrusion. Video-enhanced DIC light microscopy was superior to dark-field microscopy in visualizing the surface of these bulges. For *T. denticola*, PFs are evidently exposed at the tip of the protrusions, allowing particles to attach and rotate. *T. denticola* protrusions often appear frayed at the tip, with the membrane surface partially disrupted (Fig. 2b). Immunological techniques suggest surface exposure of PF antigens in both *T. pallidum* and *B. burgdorferi* (7, 18, 46).

The function of protrusions in spirochetes is not understood. Conceivably, protrusion formation could be an accidental result of cell division, as suggested by Listgarten and Socransky (31). Alternatively, protrusion formation could

result from an adaptive response. *T. denticola* cells fail to translate in a pure liquid medium and require a gellike medium for translation (41). However, we have observed translation of *T. denticola* in a nongellike medium for cells possessing a trailing, gyrating protrusion (42). Thus, protruding PFs might provide spirochetes with an alternative mode of motility in a manner somewhat analogous to the two forms of flagella of *Vibrio parahaemolyticus* (2). We expect that future experiments will better define the role of flagellar protrusions in the motility of spirochetes.

ACKNOWLEDGMENTS

We thank R. C. Johnson for encouragement, help, and strains, and we thank the National Institute of Occupational Safety and Health and D. Berry for use of an electron microscope. We acknowledge the assistance of the Guelph Regional STEM Facility.

This research was supported by Public Health Service grants DE04645 and AI29743, by the Rowland Institute for Science, by Biomedical Research Support grant S07-RR05433-29 awarded to West Virginia University, and by the University of Minnesota Graduate School. J. D. Ruby was supported by Physician Scientist Award K11-DE00257 from the U.S. Public Health Service.

ADDENDUM IN PROOF

We recently observed helical protrusions with wave propagation on *T. denticola* FM, *Treponema refringens*, *S. aurantia* M1, *Borrelia hermsii*, and *Borrelia parkeri*. These results suggest that the conclusions drawn from the results with *T. phagedenis*, *T. denticola* ATCC 33520, and *B. burgdorferi* 297 are likely to apply to several other spirochete strains and species.

REFERENCES

1. **Barbour, A. G.** 1984. Isolation and cultivation of Lyme disease spirochetes. Yale J. Biol. Med. **32**:818–824.
2. **Belas, R. M., M. Simon, and M. Silverman.** 1986. Regulation of lateral flagella gene transcription in *Vibrio parahaemolyticus*. J. Bacteriol. **167**:210–218.
3. **Berg, H. C.** 1976. How spirochetes may swim. J. Theor. Biol. **56**:269–273.
4. **Berg, H. C., D. B. Bromley, and N. W. Charon.** 1978. Leptospiral motility. Symp. Soc. Gen. Microbiol. **28**:285–294.
5. **Berg, H. C., and L. Turner.** 1979. Movement of microorganisms in viscous environments. Nature (London) **278**:349–351.
6. **Blair, D.** 1990. The bacterial flagella motor. Semin. Cell Biol. **1**:75–85.
7. **Blanco, D. R., J. D. Radolf, M. A. Lovett, and J. N. Miller.** 1986. The antigenic interrelationship between the endoflagella of *Treponema phagedenis* biotype Reiter and *Treponema pallidum*, Nichols strain. I. Treponemicidal activity of cross-reactive endoflagellar antibodies against *T. pallidum*. J. Immunol. **137**:2973–2979.
8. **Block, S. M., D. F. Blair, and H. C. Berg.** 1989. Compliance of bacterial flagella measured with optical tweezers. Nature (London) **338**:514–517.
9. **Block, S. M., K. A. Fahrner, and H. C. Berg.** 1991. Visualization of bacterial flagella by video-enhanced light microscopy. J. Bacteriol. **173**:933–336.
10. **Bromley, D. B., and N. W. Charon.** 1979. Axial filament involvement in the motility of *Leptospira interrogans*. J. Bacteriol. **137**:1406–1412.
11. **Canale-Parola, E.** 1978. Motility and chemotaxis of spirochetes. Annu. Rev. Microbiol. **32**:69–99.
12. **Canale-Parola, E.** 1984. The spirochetes, p. 38–70. *In* N. R. Krieg and J. G. Holt (ed.), Bergey's manual of systematic bacteriology, vol. 1. The Williams & Wilkins Co., Baltimore.
13. **Carleton, O., N. W. Charon, P. Allender, and S. O'Brien.** 1979. Helix handedness of *Leptospira interrogans* as determined by scanning electron microscopy. J. Bacteriol. **137**:1413–1416.
14. **Charon, N. W., G. R. Daughtry, R. S. McCluskey, and G. N. Franz.** 1984. Microcinematographic analysis of tethered *Leptospira illini*. J. Bacteriol. **160**:1067–1073.
15. **Charon, N. W., S. F. Goldstein, K. Curci, and R. J. Limberger.** 1991. The bent-end morphology of *Treponema phagedenis* is associated with short, left-handed periplasmic flagella. J. Bacteriol. **173**:4820–4826.
16. **Charon, N. W., C. W. Lawrence, and S. O'Brien.** 1981. Movement of antibody-coated latex beads attached to the spirochete *Leptospira interrogans*. Proc. Natl. Acad. Sci. USA **78**:7166–7170.
17. **Cockayne, A., M. J. Bailey, and C. W. Penn.** 1987. Analysis of sheath and core structures of the axial filament of *Treponema pallidum*. J. Gen. Microbiol. **133**:1397–1407.
18. **Coleman, J. L., and J. L. Benach.** 1989. Identification and characterization of an endoflagellar antigen of *Borrelia burgdorferi*. J. Clin. Invest. **84**:322–330.
19. **DeLemater, E. D., M. Haanes, and R. H. Wiggall.** 1951. Studies on the life cycle of spirochetes. V. The life cycle of the Nichols nonpathogenic *Treponema pallidum* in culture. Am. J. Syph. Gonorhea Vener. Dis. **35**:164–187.
20. **Fosnaugh, K., and E. P. Greenberg.** 1988. Motility and chemotaxis of *Spirochaeta aurantia*: computer-assisted motion analysis. J. Bacteriol. **170**:1768–1774.
21. **Fosnaugh, K., and E. P. Greenberg.** 1989. Chemotaxis mutants of *Spirochaeta aurantia*. J. Bacteriol. **171**:606–611.
22. **Francis, C. D., N. W. Charon, A. Theirmann, and C. Bolin.** 1989. Movement of latex beads on *Leptospira interrogans* serovar *pomona* mediated by monoclonal antibodies, abstr. I-123, p. 238. Abstr. 89th Annu. Meet. Am. Soc. Microbiol. 1989. American Society for Microbiology, Washington, D.C.
23. **Goldstein, S. F., and N. W. Charon.** 1988. The motility of the spirochete *Leptospira*. Cell Motil. Cytoskeleton **9**:101–110.
24. **Goldstein, S. F., and N. W. Charon.** 1990. Multiple exposure photographic analysis of a motile spirochete. Proc. Natl. Acad. Sci. USA **87**:4895–4899.
25. **Hampp, E. G.** 1946. Morphologic alteration of smaller oral treponemes during aging of cultures; effect of age on viability of spirochetal cultures. J. Am. Dent. Assoc. **33**:201–206.
26. **Hampp, E. G., D. B. Scott, and R. W. G. Wyckoff.** 1948. Morphologic characteristics of certain cultured strains of oral spirochetes and *Treponema pallidum* as revealed by the electron microscope. J. Bacteriol. **56**:755–769.
27. **Holt, S. C.** 1978. Anatomy and chemistry of spirochetes. Microbiol. Rev. **42**:114–160.
28. **Kreiling, J. A., and N. W. Charon.** 1991. Characterization of periplasmic flagella of *Borrelia burgdorferi* by high-magnification dark-field microscopy, abstr. I-87, p. 205. Abstr. 91st Gen. Meet. Am. Soc. Microbiol. 1991. American Society for Microbiology, Washington, D.C.
29. **Leschine, S. B., and E. Canale-Parola.** 1980. Rifampin as a selective agent for isolation of oral spirochetes. J. Clin. Microbiol. **12**:792–795.
30. **Limberger, R. J., and N. W. Charon.** 1986. *Treponema phagedenis* has at least two proteins residing together on its periplasmic flagella. J. Bacteriol. **166**:105–112.
31. **Listgarten, M. A., and S. S. Socransky.** 1964. Electron microscopy of axial fibrils, outer envolope, and cell division of certain oral spirochetes. J. Bacteriol. **88**:1087–1103.
32. **Macnab, R. M.** 1987. Flagella, p. 70–83. *In* F. C. Neidhardt, J. L. Ingraham, K. B. Low, B. Magasanik, M. Schaechter, and H. E. Umbarger (ed.), *Escherichia coli* and *Salmonella typhimurium*: cellular and molecular biology. American Society for Microbiology, Washington, D.C.
33. **Macnab, R. M.** 1990. Genetics, structure, and assembly of the bacterial flagellum. Symp. Soc. Gen. Microbiol. **46**:77–106.
34. **Macnab, R. M., and S.-I. Aizawa.** 1984. Bacterial motility and the bacterial flagellar motor. Annu. Rev. Biophys. Bioeng. **13**:51–83.
35. **Morton, H. E., G. Rake, and N. R. Rose.** 1951. Electron microscope studies of treponemes. III. Flagella. Am. J. Syph. Gonorrhea Vener. Dis. **35**:503–516.
36. **Mudd, S., K. Polevitsky, and T. F. Anderson.** 1943. Bacterial

morphology as shown by the electron microscope. J. Bacteriol. **46**:15–24.
37. **Noguchi, H.** 1911. A method for the pure cultivation of pathogenic *Treponema pallidum* (*Spirochaeta pallida*). J. Exp. Med. **14**:99–108.
38. **Noguchi, H.** 1912. Cultural studies on mouth spirochaetae (*Treponema microdentium* and *macrodentium*). J. Exp. Med. **15**:81–89.
39. **Noguchi, H.** 1926. Abnormal bacteria flagella in cultures. J. Am. Med. Assoc. **86**:1327–1329.
40. **Paster, B. J., F. E. Dewhirst, W. G. Weisburg, L. A. Tordoff, G. J. Fraser, R. B. Hespell, T. B. Stanton, L. Zablen, L. Mandelco, and C. R. Woese.** 1991. Phylogenetic analysis of the spirochetes. J. Bacteriol. **173**:6101–6109.
41. **Pietrantonoio, F., P. B. Noble, R. Amsel, and E. C. S. Chan.** 1988. Locomotory characteristics of *Treponema denticola*. Can. J. Microbiol. **34**:748–752.
42. **Ruby, J. D., K. Curci, S. F. Goldstein, and N. W. Charon.** 1991. Evidence that the periplasmic flagella of *Treponema denticola* and *Treponema phagedenis* can be external, abstr. I-86, p. 204. Abstr. 91st Gen. Meet. Am. Soc. Microbiol. 1991. American Society for Microbiology, Washington, D.C.
43. **Silverman, M. R., and M. I. Simon.** 1974. Flagellar rotation and the mechanism of bacterial motility. Nature (London) **249**:73–74.
44. **Smibert, R. M.** 1984. Genus III. *Treponema* Schaudinn 1905, 1728^{AL}, p. 49–57. *In* N. R. Krieg and J. G. Holt (ed.), Bergey's manual of systematic bacteriology, vol. 1. The Williams & Wilkins Co., Baltimore.
45. **Smith, D. T.** 1932. Oral spirochetes and related organisms, p. 1–243. *In* Fuso-spirochetal diseases. The Williams & Wilkins Co., Baltimore.
46. **Stamm, L. V., and P. J. Bassford, Jr.** 1982. Cellular and extracellular protein antigens of *Treponema pallidum* synthesized during in vitro incubation of freshly extracted organisms. Infect. Immun. **47**:799–807.
47. **Taylor, G.** 1952. The action of waving cylindrical tails in propelling microscopic organisms. Proc. R. Soc. London Ser. A **211**:225–239.
48. **Van Weelden, G. J., N. W. Charon, and S. J. Norris.** 1990. Viscosity and the motility of *Treponema phagedenis* and *Treponema pallidum*, abstr. I-76, p. 211. Abstr. 90th Annu. Meet. Am. Soc. Microbiol. 1990. American Society for Microbiology, Washington, D.C.
49. **Woese, C. R.** 1987. Bacterial evolution. Microbiol. Rev. **51**:221–271.